Physics of the Earth and Planetary Interiors, 10 (1975) 299–312

MORPHOLOGY OF SLOWLY-VARYING GEOMAGNETIC EXTERNAL FIELDS – A REVIEW

S. MATSUSHITA

High Altitude Observatory of NCAR, Boulder, Colo. (U.S.A.)

(Accepted for publication February 27, 1975)

The morphology of slowly-varying geomagnetic external fields (such as Sq, L, and Dst) and the production mechanisms of electric current systems for those fields are briefly reviewed to provide background knowledge of the present state of research regarding the source fields for scientists concerned with the electromagnetic induction within the earth. It is concluded that both the Sq and Dst fields seem to have sources both in the magnetosphere and the ionosphere, while the classic idea of L-field production solely in the ionosphere by the wind dynamo is still acceptable.

1. Introduction

The present review paper is prepared to outline briefly the current stage of research on slowly-varying source fields in order to assist in the investigation of the electromagnetic induction within the earth. Because of the page limitation, referenced papers are mostly recent interesting publications within the past five years. Even with this restriction more than seventy references are needed to cover the vast research area from the lower ionosphere through the magnetosphere, including the interplanetary field effects. Interested readers are advised to examine the referenced papers and the references therein for specifics concerning the subject matter.

Electric currents responsible for the external part of geomagnetic solar quiet (Sq) and lunar (L) daily variations seem to flow mainly in the ionospheric dynamo region (90–150 km altitude), although some amount may flow along the earth's magnetic field lines from the dynamo region in one hemisphere to the other. Other magnetospheric electric currents (such as front magnetopause, tail, and quiet-time ring currents) by themselves alone are not sufficient to produce the Sq field, although the magnetosphere plays an important role in producing the Sq current system in the dynamo region as discussed in Section 2. Rocket measurements of the earth's magnetic field (e.g. Yabuzaki and Ogawa, 1974), solar flare and eclipse effects on geomagnetic and ionospheric variations, and the height distribution of electric conductivity are the best evidence available for a dynamo-region source of Sq and L electric currents. However, the production mechanism of the currents, particularly for Sq, is the subject of one of the most important ongoing investigations (Matsushita, 1974). The major part of the present report is centered on this exciting topic.

Concerning the Dst field, recent investigations show that this field is not produced by simple doughnut-shaped westward electric currents at about four earth radii from the earth's center in the equatorial plane, but probably by a complicated system of partial rings and field-aligned currents associated with substorms. Moreover, some evidence of midlatitude ionospheric contributions to the Dst field is gradually being accumulated. These are briefly discussed in Section 4.

2. Sq field

Equivalent overhead (external) electric current systems for the solar quiet (Sq) daily geomagnetic variation field have been estimated from the ground-based geomagnetic data by various scientists (e.g. Matsushita, 1967a, 1968; and the references therein). Using the same IGY data analyzed by Matsushita and

Maeda (1965), Suzuki (1973b) has recently obtained Sq current systems without the equatorial electrojet, since the intense jet in a narrow equatorial region may cause difficulties for the spherical harmonic approximation. Suzuki's study shows a 10–20% smaller external current intensity than that of Matsushita and Maeda, but the difference of the internal current intensity is not consistent, the former sometimes being greater and at other times smaller than the latter with about 50% probability.

Concerning the Sq equivalent current system in the polar region named Sq^p, Matsushita et al. (1973) have estimated it for each month of 1965 by the spherical harmonic analysis (order m = 1 to 4, and degree $n=m$ to $m+15$) of 2.5-min digitized geomagnetic data from 40 stations located from the northern polar cap through the southern subauroral zone. To obtain a better spherical harmonic fit to the data in the polar region, equatorial and auroral electrojet effects have been minimized through smoothing techniques. Equivalent external and internal electric current systems of Sq (= Sq^p + Sq^o) and of Sq^o (smooth extrapolation of midlatitude Sq to the pole) for May and June 1965 are shown in Fig. 1. It can be noticed that the midlatitude current intensity is enhanced by including Sq^p, in the same way it is enhanced by in-

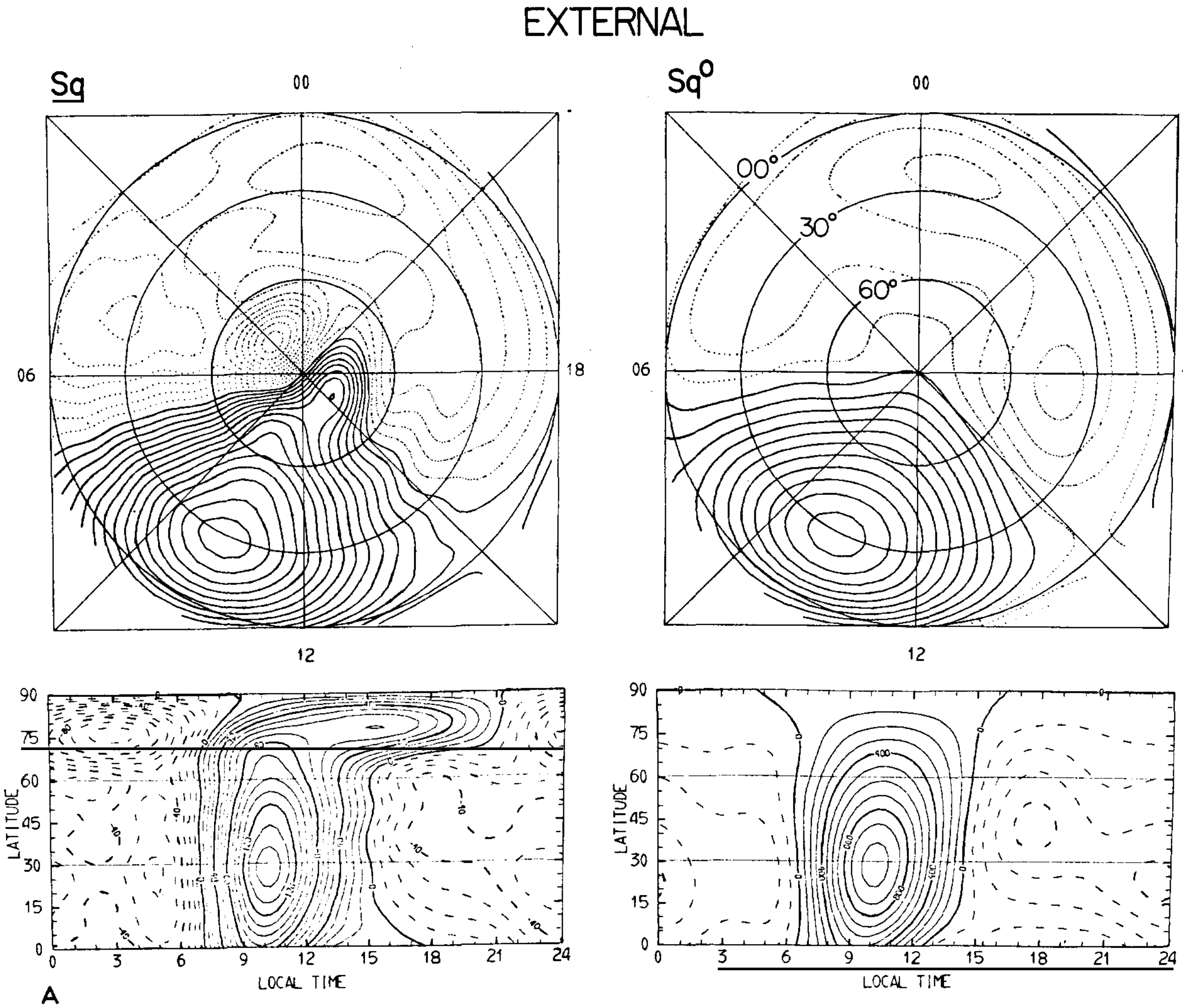

Fig. 1A. For caption see p. 301.

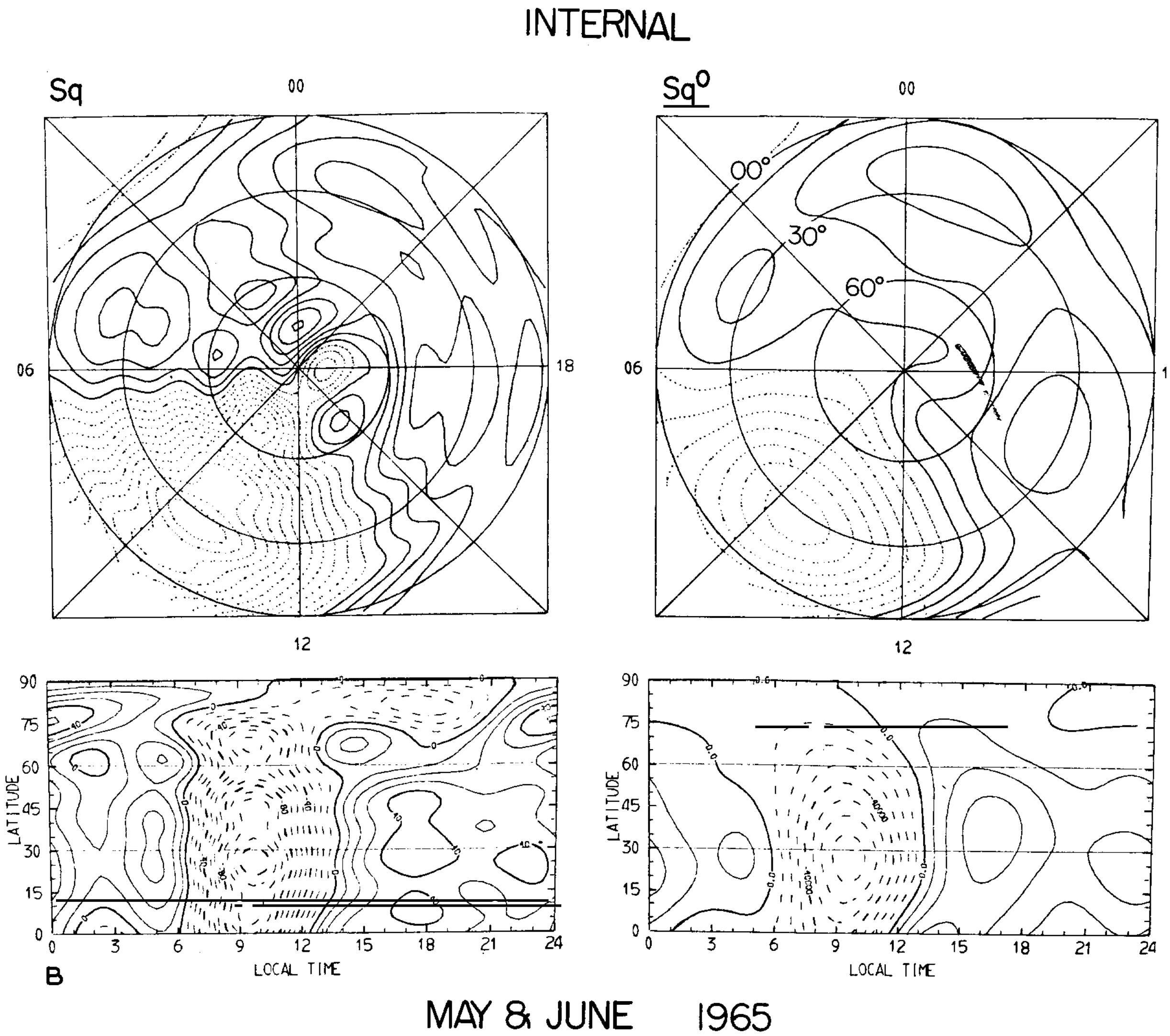

Fig. 1. Equivalent external (Fig. 1A) and internal (Fig. 1B) electric current systems of Sq (left) and Sq^0 (right), which have been estimated from the northward and vertical components of quiet-time geomagnetic variation fields observed at 40 stations in May and June 1965, are presented in polar (top) and rectangular (bottom) coordinates with respect to geomagnetic latitudes and local times. The solid (broken) curves show counterclockwise (clockwise) current flows with a contour interval of 10^4 A.

cluding the equatorial electrojet (Suzuki, 1973b).

The main coefficients for May and June in 1965 compared with those obtained earlier are listed in Table I. The amplitudes C_n^m and the phase angles α_n^m for Sq and Sq^0 for May–June 1965 are almost the same for odd harmonic terms but differ for even terms. Also, the first two terms of the amplitude ratio of the external to the internal component E_n^m/I_n^m are different between Sq and Sq^0, although the phase difference remains almost the same. These listed values for May and June in Table I are from the northward and downward geomagnetic components. The results from the eastward and downward geomagnetic components are similar to the listed values except slightly smaller in amplitude. Also, the spherical harmonic terms during disturbed periods are fairly similar to the values for quiet periods, except for an increase in C_n^m.

TABLE I

Comparison of spherical harmonic terms

Year		1902	*	1932–1933	May–June 1965		1902	*	1932–1933	May–June 1965	
Sunspot number		5	6	8	20		5	6	8	20	
m	n				Sq	Sq$^{\mathrm{o}}$				Sq	Sq$^{\mathrm{o}}$
		Amplitude $C_n^m(\gamma)$:					*Phase angle* $\alpha_n^m(°)$:				
1	2	7.0	7.5	10.5	6.8	7.2	035	019	014	027	029
2	3	4.5	4.2	5.2	4.2	4.2	215	209	198	201	201
3	4	2.1		1.6	1.7	1.7	047		040	039	039
1	1	4.3	5.0	3.8	7.9	3.3	023	039	005	012	042
1	3	2.1	0.8	0.9	2.9	0.8	344	318	339	338	359
		Amplitude ratio E_n^m/I_n^m:					*Phase difference* $\epsilon_n^m - \iota_n^m$ (°):				
1	2	3.0	2.4	2.3	1.9	3.5	−20	−21	−09	−22	−21
2	3	2.2	2.1	2.4	6.1	3.7	−18	−13	−10	−21	−23
3	4	2.4	1.9	2.2	2.1	2.1	−21	−02	−14	−12	−22

* 1933 for C_n^m and α_n^m, and 1923 for E_n^m/I_n^m and $\epsilon_n^m - \iota_n^m$.
Note that the results, except for 1965, are for yearly, seasonal, or equinoctial average (see Matsushita, 1967a).

To explain the Sq current system, the dynamo fields and currents caused by the lowest negative order solar-diurnal tidal mode (1, −1) in the ionospheric E region, which is sometimes referred to as the (1, −2) mode (e.g. Lindzen and Chapman, 1969), have been discussed by several scientists (e.g. Matsushita, 1969, 1971, 1973; Matsushita and Tarpley, 1970; Tarpley, 1970b; Stening, 1969, 1970; Kato, 1971; Murata, 1974). An example is presented in Fig. 2A to demonstrate the Sq-like current density $\boldsymbol{J}$ and electrostatic-field distribution $\boldsymbol{Es}$ obtained from the estimated electric conductivity tensor $[\Sigma]$ and an assumed tidal wind $\boldsymbol{V}$ in the E region, using the well-known equation $\boldsymbol{J} = [\Sigma](\boldsymbol{V} \times \boldsymbol{B} + \boldsymbol{Es})$ where $\boldsymbol{B}$ is the main magnetic field of the earth with conditions $\nabla \cdot \boldsymbol{J} = 0$ and $\nabla \times \boldsymbol{Es} = 0$. Stening (1969, 1970) examined seasonal effects and longitudinal inequalities by varying $[\Sigma]$ and $\boldsymbol{B}$ values, and Murata (1974) emphasized vertical electric current effects.

Although (1, −1) seems to be the main tidal mode required for Sq, other minor tidal modes may be superposed. For example, Schieldge et al. (1973) simulated an Sq current pattern for 5 August 1958 by superposing semidiurnal tidal modes on (1, −1). Richmond (1973a,b) showed that the height-varying winds similar in structure to the (1,1) tidal mode give a considerable effect on the day-to-day variations of the near-equatorial geomagnetic field. Richmond (1974) also suggested that for some tidal modes, such as (2,3), effects of field-aligned electric currents between the northern and southern hemispheres need to be considered. Volland and Mayr (1972, 1973, 1974) discussed theoretically the general behavior of three-dimensional tidal modes in the thermosphere.

If the (1, −1) tidal mode is not predominant in the dynamo region, an alternative suggestion for the Sq currents has been given by Matsushita (1971, 1972), who suggested that the necessary midlatitude electric field in the dynamo region is produced originally by a plasmaspheric motion and is mapped down along the earth's magnetic field lines, and that the high-latitude electric field is produced originally by the interaction between the solar wind and the magnetosphere. Although further details of this mechanism need to be examined, these plasmaspheric and magnetospheric effects on the dynamo region can not be ignored (Stening, 1973).

In order to select the best model among these suggested mechanisms of the Sq-current production, the assumed amplitudes and phase angles of tidal modes in the dynamo region and the electrostatic-field distribution at various latitudes need to be compared with observed results of winds and fields. As reviewed by Matsushita (1973) and Matsushita and Mozer (1973), measurements of chemiluminous clouds (such as TMA) released by rockets show the E-region wind shears, but provide almost no information in the daytime (lithium clouds show promise of daytime wind observations in the future). Radar observations of meteor trail motions, laser-radar measurements of nighttime atmospheric density variations, and incoherent-scatter radar observations of plasma drifts provide further information about upper atmospheric winds. The incoherent scatter radar observations of the tidal winds at St. Santin (g.g. 44.7°N, 2.2°E) in summer and winter indicated a diurnal component at 100–450-km altitude, and a semidiurnal component with a mode of (2,4) at 100–135-km altitude and (2,2) at 135–225 km (Amayenc and Reddy, 1972). Also, observed results of the meridional winds at St. Santin (Amayenc, 1974) in the spring equinox agreed fairly well with the height distributions of (1, −1) and (2,2) tides theoretically estimated by Volland and Mayr (1973). However, in the dynamo region the diurnal wind speed is not particularly greater than the semidiurnal, and the phases of both diurnal and semidiurnal components change greatly with height.

Based on the meteor radar observations at Garchy near St. Santin, Fellous et al. (1974) found evanescent modes of the diurnal tide and higher-order modes of the semidiurnal tide. Bernard (1974) examined the tidal observations by the meteor radar at Garchy and by the incoherent-scatter measurements at St. Santin, and concluded that the semidiurnal tide at 80–100-km altitude range changes greatly, even from one day to the next, but the (2,4) mode is dominant at altitudes higher than 100 km. Using laser radar, meteor radar, and

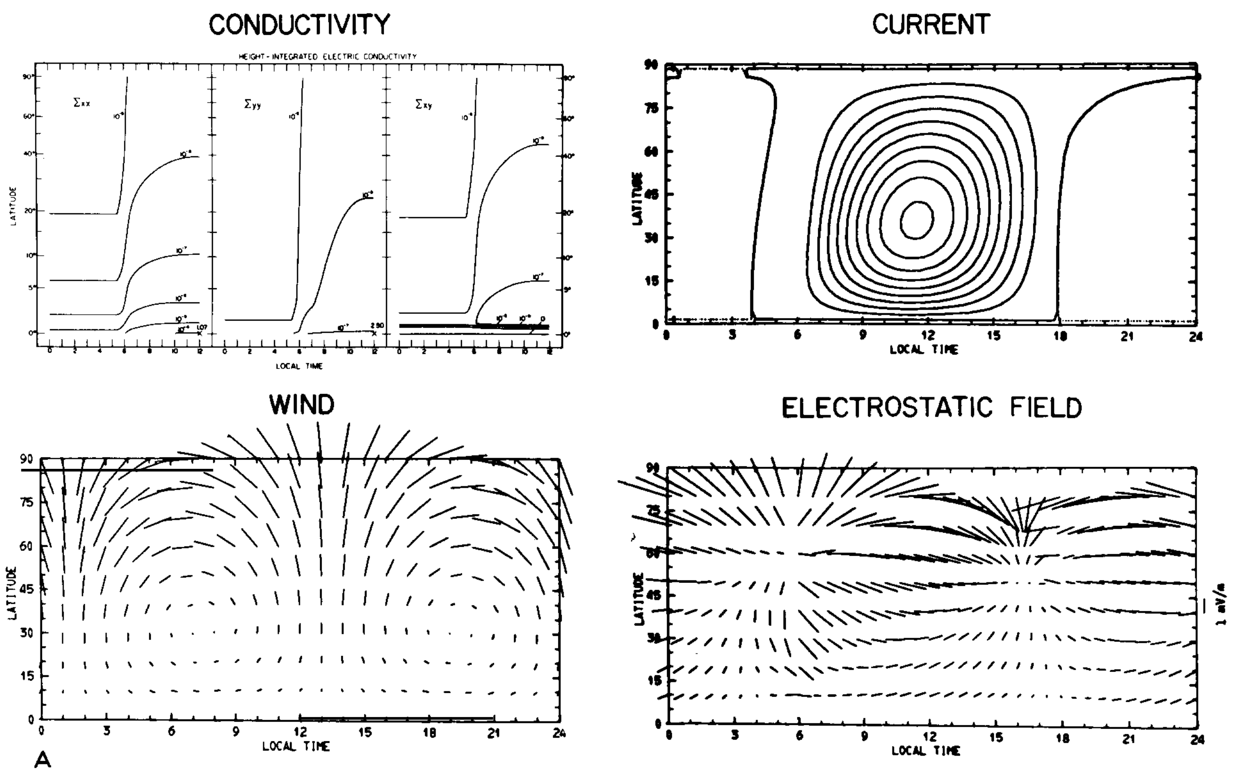

Fig. 2A. Top left: contours of height-integrated anisotropic electric conductivities Σ_{xx}, Σ_{yy}, and Σ_{xy} in units of e.m.u. for 00–12 h (symmetric with respect to the noon meridian). Bottom left: wind vectors for the solar (1,−1) tidal mode. The lengths equal to 5° latitude correspond to 50-m/sec wind speed. Top right: Sq counterclockwise current system calculated from the conductivity and the wind models shown at the left. The current intensity between two consecutive lines is 10^4 A. Bottom right: electrostatic field distribution plotted in 10° steps of latitude and longitude (after Matsushita, 1971).

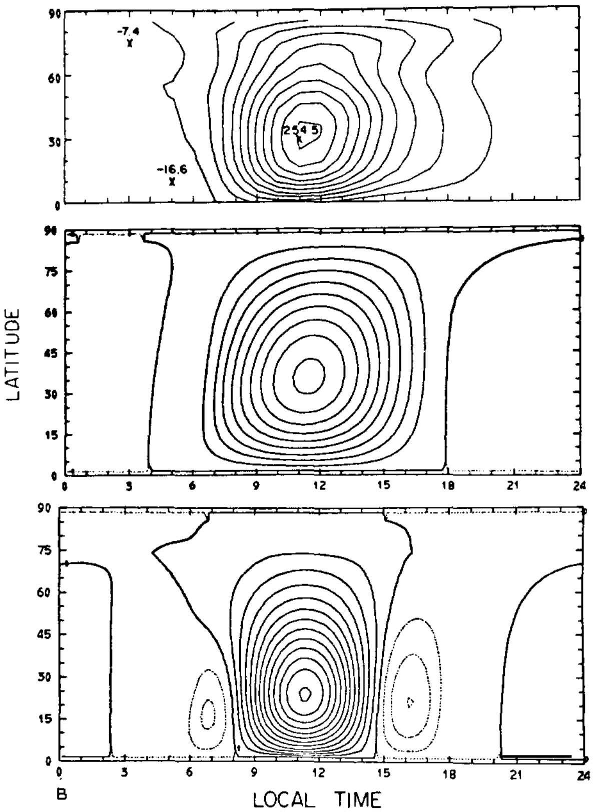

Fig. 2B. The yearly-average Sq current during the IGY (top) is compared with the current obtained from the (1,−1) tidal mode (middle) and that from the (2,2) mode (bottom). The current intensity between two consecutive lines is $2.5 \cdot 10^4$ A for the top diagram and 10^4 A for the two others.

radio sounding techniques, at Kingston, Jamaica (g.g. 18°N, 77°W), Alleyne et al. (1974) found that there exists a diurnal oscillation with a vertical wavelength of about 15 km, accompanied by a semidiurnal oscillation with a much longer vertical wavelength, in the atmosphere between 70 and 170 km altitude. The vertical wavelength of the observed diurnal oscillation does not correspond to the theorized (1, −1) and (1,1) modes. Thus, wind observations at present do not particularly indicate a predominant and consistent (1, −1) tide in the dynamo region, which is an essential tidal wind to produce the Sq-current system, although they show semidiurnal modes, especially (2,4).

The other way to examine production models of the Sq-current system is by the electrostatic-field distribution which can be observed by different methods, such as $E \times B$ drifts of barium clouds released by rockets, probe measurements by space vehicles (satallites, rockets, and balloons), and $E \times B$ plasma drifts measured by incoherent-scatter radars. Ten to twenty barium releases at midlatitudes showed the electrostatic field around dawn and dusk (see Matsushita, 1972). However, it is very difficult to compare the electrostatic field estimated from the Sq around dawn and dusk with those barium results, since the electric field can change rapidly, due to sharp conductivity changes, and the superposed local winds caused by a strong temperature gradient may be important at these times. Probe observations of the electrostatic field by balloons, rockets, and satellites have been made mainly at high latitudes (see Matsushita and Mozer, 1973; and the references therein).

Horizontal $E \times B$ drifts in the ionospheric E and F regions observed by the incoherent-scatter radar system at Millstone Hill (g.g. 42.6°N, 71.5°W) showed semidiurnal variations (Evans, 1972a,b), but more recent observations of the F region showed the dominance of a diurnal variation (Kirchhoff and Carpenter, 1975). Also, F-region diurnal winds deduced from St. Santin (g.g. 44.7°N, 2.2°E) data showed a better theoretical agreement when a *diurnal* electric field from the dynamo region was taken into consideration during summer and equinoxes (Amayenc and Vasseur, 1972). A diurnal $E \times B$ drift at F-region heights over Malvern (g.g. 51.2°N, 2.3°W) was reported by Taylor (1974), but a terdiurnal $E \times B$ drift of the F-region plasma superposed on a diurnal drift at Arecibo (g.g. 18.3°N, 66.8°W) was found by Behnke and Harper (1973), while Jicamarca (g.g. 12.0°S, 76.9°W) clearly showed a predominant diurnal variation (e.g. Woodman, 1970; Balsley, 1973). Using the whistler method of tracking cross-field plasma drifts in the magnetosphere during quiet periods, Carpenter and Seely (1974, 1975) found that the observed E–W electric field agrees well with Evans' Millstone Hill measurement in the daytime and with Kirchhoff and Carpenter's at night.

These observations can be compared with the theoretical electrostatic-field distributions estimated with different assumptions by various scientists. Maeda (1955, 1963) semiempirically estimated the electrostatic field for Sq during the Second Polar Year (1932–1933) and computed its effect on the F-region drift. Matsushita (1969) and Matsushita and Tarpley (1970) obtained the electrostatic field for Sq at the equinoxes

TABLE II

Electric field reversal time*

		N → S	S → N	W → E	E → W	Reported by
(1)	Millstone Hill dip lat. 57°	09 and (21)	(03) and 15	07 and 19	(01) and 13	Evans (1972a)
	geog. lat. 43°N	02 and (08)	(05) and 14	19	12	Kirchhoff and Carpenter (1975)
	Malvern dip lat. 50° geog. lat. 52°N				11.5	Taylor (1974)
	Wind dynamo for about 50°N	01 and 09	03 and 21	03 and 21	01 and 11	Maeda (1955, 1963)
		01	15	06	16	Matsushita (1969, 1972), Matsushita and Tarpley (1970)
		10	16	7.5	17.5	Stening (1973)
		16	19.5	09 and 17	14 and 21	Schieldge et al. (1973)
		09	23	03	15	Murata (1974)
	Plasmaspheric dynamo for about 50°N	03	13	22	10	Matsushita (1971, 1972)
		08	15	17 or 23	09	Stening (1973)
(2)	Arecibo dip lat. 30°			03	14	Harper (1971, in Stening, 1973)
	geog. lat. 18°N			01, 08, and (17)	05, 15, and (21)	Behnke and Harper (1973)
	Wind dynamo for 20–30°N			05 or 23	13	Maeda (1955, 1963)
				3.5	17	Matsushita (1969, 1972)
				05	20	Stening (1973)
				07	22.5	Schieldge et al. (1973)
				03	15	Murata (1974)
	Plasmaspheric dynamo for 20–30°N			01	14	Matsushita (1971, 1972)
				04 and 17	14 and 19	Stening (1973)
(3)	Jicamarca dip lat. 01° geog. lat. 12°S			07	20	Woodman (1970), Balsley (1973)
	Wind dynamo around the equator**			05	19	Maeda (1955, 1963)
				04	18	Matsushita (1969, 1972*)
				06	20	Stening (1973)
				06	23	Schieldge et al. (1973)
				03	15	Murata (1974)
				07	22.5	Matuura (1974)

* Reversal times in parentheses are less reliable.

** Plasmaspheric dynamo results are the same at the equator.

from the assumption of a (1, −1) tidal mode (see Fig. 2A), and Matsushita (1972) presented the field effect on the F-region drift. Stening (1973) examined seasonal variations and longitudinal inequalities of the field by changing the electric conductivity and the earth's magnetic main field, while Murata (1974) included the vertical current; both of these contained the same assumption of the (1, −1) tidal mode. Schieldge et al. (1973) obtained the field from four assumed tidal modes, (1, −1), (2,2), (2,3), and (2,4). Concerning the alternative model of the Sq-current formation caused by the electric field produced in the plasmasphere, Matsushita (1971, 1972) presented the field distributions in the dynamo region and in the F level, and Stening (1973) showed the fields in different seasons.

The electrostatic fields (or $\boldsymbol{E} \times \boldsymbol{B}$ drifts) estimated from all these theoretical models are compared with those observed by the incoherent-scatter radar facilities in order to identify the best model. A comparison with regard to the change-over time of the NS and EW directions of the field is listed in Table II. Observations at Chatanika (g.g. 64.9°N, 147.7°W) are ignored since these observed results usually show disturbance effects. As seen in Table II, none of the theoretical results ideally agrees with the observations. When a small amount of time lag is allowed, the plasmaspheric-dynamo model seems to show a better agreement than the wind-dynamo model, in spite of fairly detailed adjustments for winds, conductivities, vertical currents, etc., although either model is satisfactory for the equatorial region. The most reasonable suggestion is that the Sq current in the dynamo region is produced partly by the electric field originating in the plasmasphere–magnetosphere and partly by the semidiurnal wind dynamo (particularly in the daytime), including the F-layer diurnal wind dynamo (Rishbeth, 1971; Matuura, 1974). In fact, the current system and electrostatic-field distribution obtained for L by the (2,2) mode (right diagram of fig. 10 in Matsushita, 1969), where 10 times larger current intensity and electric field are plausible for Sq, strongly support this idea of a semidiurnal wind dynamo (see Fig. 2B). Kirchhoff and Carpenter (1975) presented a similar suggestion, while Behnke and Hagfors (1974) inferred that the daytime electric fields are caused by the E-region wind dynamo and the nighttime fields are by the F-layer dynamo due to thermospheric winds. In fact, S. Fukao (private communication, 1974) has showed theoretically that the F-layer wind dynamo produces large electrostatic fields at night. He has also examined the effects of the magnetospheric dawn-to-dusk electric field. Although Pratap et al. (1973) discussed a three-dimensional dynamo theory including magnetospheric effects, the problem needs to be examined in much more detail taking into consideration all regions from the upper mesosphere through the outer magnetosphere.

For the scientists interested in electromagnetic induction, the real source of the Sq current may not be particularly important. However, in addition to the field-aligned current effects on Sq, there are some other effects which cannot be explained by dynamo-region currents. As was discussed by Matsushita et al. (1973), the interplanetary magnetic field (IMF) sector structures, such as "toward" the sun with a westward field component and "away" from the sun with an eastward field, cause not only a clear change of the Sq^p-current system over the polar region but also a remarkable shift of the Sq-current focus. Corresponding to the IMF toward (away) sector structure, the Sq-current focus moves equatorward (poleward) by about 4°. This effect is probably caused by the plasmaspheric expansion (contraction), instead of westward (eastward) electric currents in the dynamo region, due to the IMF toward (away) sector structure. In spherical harmonic analyses, incidentally, these sector effects are presented by the sign reversal of the C_1^0 term.

Tarpley (1973) suggested that seasonal movements of the Sq-current foci indicate an asymmetric wind system between the northern and southern hemispheres even during equinoxes, and Matsushita (1967a) discussed that the Sq day-to-day changes are caused partly by the wind system and partly by small disturbance effects. The IMF sector effects may correspond to the "small disturbance" and play an important role in seasonal and day-to-day changes of the Sq field. The shift of the equivalent overhead Sq^p-current system with the IMF sector changes may be inferred from the distorted magnetospheric electric fields which map down along the earth's magnetic field lines and produce a distorted Sq^p-current system in the dynamo region.

Concerning the equatorial zone, all theoretical models agree approximately with Jicamarca observations as shown in Table II. Also, the F-region vertical motion caused by the electric field measured by barium clouds over Thumba showed a fairly good agreement with those observed by Jicamarca radar (Balsley, 1973). Returning flow of the equatorial electrojet currents was discussed by Suzuki (1973a), and the so-called counter-electrojet (which causes an occasional steep decrease of the geomagnetic H component below its nighttime level in the early afternoon on a quiet day) was examined by several researchers (e.g. Hutton and Oyinloye, 1970; Onwumechili and Akasofu, 1972; Fambitakoye et al., 1973; Rastogi, 1974). If this phenomenon is free from any storm or lunar tidal effects, it may be explained by the higher harmonics of atmospheric tides, such as the (2,2) or (2,4) mode. Since vertical propagation conditions for these tidal modes may vary day by day, it is no surprise that this phenomenon occurs only occasionally. Also, it must be noted that changes in the electric field and wind at non-equatorial latitudes almost immediately affect the equatorial electric field in the dynamo region, because the equatorial field is produced as an integrated result of the dynamo mechanism in a wide non-equatorial area. Accordingly, electrostatic fields produced at plasmaspheric and F2 low latitudes may map down to the dynamo region at midlatitudes along magnetic-field lines, and then change the equatorial electric field in the dynamo region. This effect may also contribute to the cause of the counter-electrojet phenomenon.

3. L field

The equivalent overhead (external) electric current system for the lunar (L) daily geomagnetic variation field was estimated from the ground-based geomagnetic data when the daily mean was taken as the zero level (Matsushita, 1967a, 1968; and the references therein), and also when the current intensity at solar midnight was assumed to be zero, taking into consideration the solar daily variation of the electric conductivity (Matsushita, 1969) as shown in the top of Fig. 3. Detailed studies of the L field from the data at 100 observatories for the interval 1957.5–1960.0, eliminating the contribution of the sea-tidal dynamo, were conducted by Malin (1973), whose result was surprisingly similar to the current system obtained from a much simpler procedure by Matsushita (1969).

To explain the L-current system, the dynamo fields and currents caused by the lunar semidiurnal (2,2) tidal mode in the dynamo region were discussed by Matsushita (1969) and Tarpley (1970a), and the electrostatic-field distribution for L was estimated by Matsushita and Tarpley (1970), as presented in the middle and bottom diagrams of Fig. 3. The $\boldsymbol{E} \times \boldsymbol{B}$ drifts in the ionospheric F layer caused by the dynamo-region electrostatic field were obtained by Matsushita (1972). All these theoretical estimations seem to be satisfactory on the basis of indirect evidence, such as

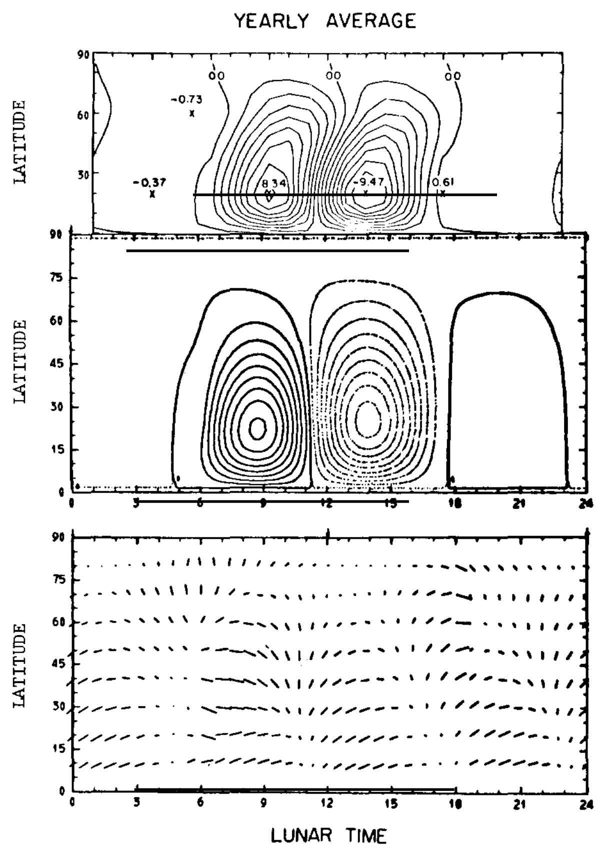

Fig. 3. Yearly averaged L external current system estimated from geomagnetic data (top) and that calculated from the semidiurnal lunar (2,2) tidal wind model (middle) with the electrostatic-field distribution (bottom) for a new or full moon day (or luni-solar) during a moderate sunspot period. The current intensity between two consecutive lines is 10^3 A, and the vector of the electric field is plotted for each 10° step of latitude and longitude, where the lengths equal to 5° latitude correspond to 0.2 mV/m.

the ionospheric lunar variations, although direct measurements of tidal winds and electric fields caused by the lunar gravitational force are not yet available.

Using the E-region electron-drift measurements at Jicamarca (g.g. 12.0°S, 76.9°W) and the geomagnetic H data from Huancayo (g.g. 12.0°S, 75.3°W), Tarpley and Balsley (1972) investigated lunar variations in the Peruvian electrojet, and inferred from the analysis that the electric field for L, which is of the order of 0.1 mV/m, shows a clear difference between day and night and a large annual variation. Also, a convenient method of obtaining lunar semidiurnal variations of the geomagnetic field from the 2.5-min data scalings on tape was suggested by Matsushita and Campbell (1972), and the O_1 component of the geomagnetic lunar daily variation was discussed by several scientists (e.g. Winch, 1970; Tarpley, 1971). Recently there has occurred some renewed interest in the comparison of seasonal and solar-cycle variations of L with those of Sq. Appropriate application of the above-mentioned convenient method for magnetic data tape analysis could help clarify these variations.

4. Dst field

Geomagnetic variations during storms can *statistically* be divided into storm-time (measured from the beginning of the storm) and local-time dependent components. The former component has traditionally been called "storm-time variation" and designated by Dst, while the latter has been called "disturbance-daily variation" with the designation DS. The Dst has occasionally been called DR, since it has sometimes been thought that the Dst variation is caused by *ring*-shaped westward electric currents at about four earth radii from the earth's center in the equatorial plane. Also, to reemphasize the investigation of an individual storm event instead of average storm behavior, "polar substorm" has recently become a popular term, and DS has often been called DP, where P denotes *polar* substorm (for more details, see Matsushita, 1967b). Although the classic notations Dst and DS are used, for simplicity, throughout the present section, all recent conceptions are included in those notations. Since the Dst and DS fields are not completely independent and separable, particularly for the three-dimensional electric current model, the DS field is partly included in the present section.

A very extensive study of the morphology of the Dst field was conducted by Sugiura and Chapman (1960), using the geomagnetic data obtained at 26 stations for 346 storms during 44 years, 1902–1945. Also, a very useful disturbance index "hourly values of equatorial Dst" has been provided by M. Sugiura, D.J. Poros, and S.J. Cain in NASA Goddard Space Flight Center for many years. Based on this index and the auroral electrojet index AE, it has recently been suggested by several scientists (e.g. Kokubun, 1972; Kamide, 1974; Kane, 1974) that the southward component of the interplanetary magnetic field often triggers a storm occurrence or an expansion of the auroral oval region. Also, a theoretical relation between Dst and the solar wind merging electric field was discussed by Siscoe and Crooker (1974a).

Soon after the triggering action, probably due to the magnetospheric-convection electric field, protons in the Alfvén layer (inner edge of the ion sheet) in the night-side magnetosphere move earthward and increase their energy density to produce a storm-time ring current (Coroniti, 1973). Satellite observations of the storm-time ring current particles at the beginning of storms were reported by Smith and Hoffman (1974). The ring current shape may not be a symmetrically complete ring, but may involve an asymmetric ring (in regards to both geocentric distance and current intensity) and/or a few partial rings. Jaggi and Wolf (1973) discussed an asymmetric ring current, and Siscoe and Crooker (1974b) discussed theoretically the partial-ring current contribution to the Dst field.

Concerning the three-dimensional current loop of the Dst ring with field-aligned and ionospheric currents for the DS field, Fukushima and Kamide (1973a,b) reviewed various models. As shown in Fig. 4, these models may be classified into the following four types: (1) dayside partial ring current with downflowing (around dawn) and upflowing (around dusk) field-aligned currents (Akasofu and Meng, 1969); (2) nightside partial-ring current with field-aligned currents (McPherron et al., 1973); (3) tail- and partial-ring currents with field-aligned currents (Kamide and Fukushima, 1972); and (4) no-downflowing current in the nightside magnetosphere (Rostoker, 1974). Satellite observations are essential to estimate the

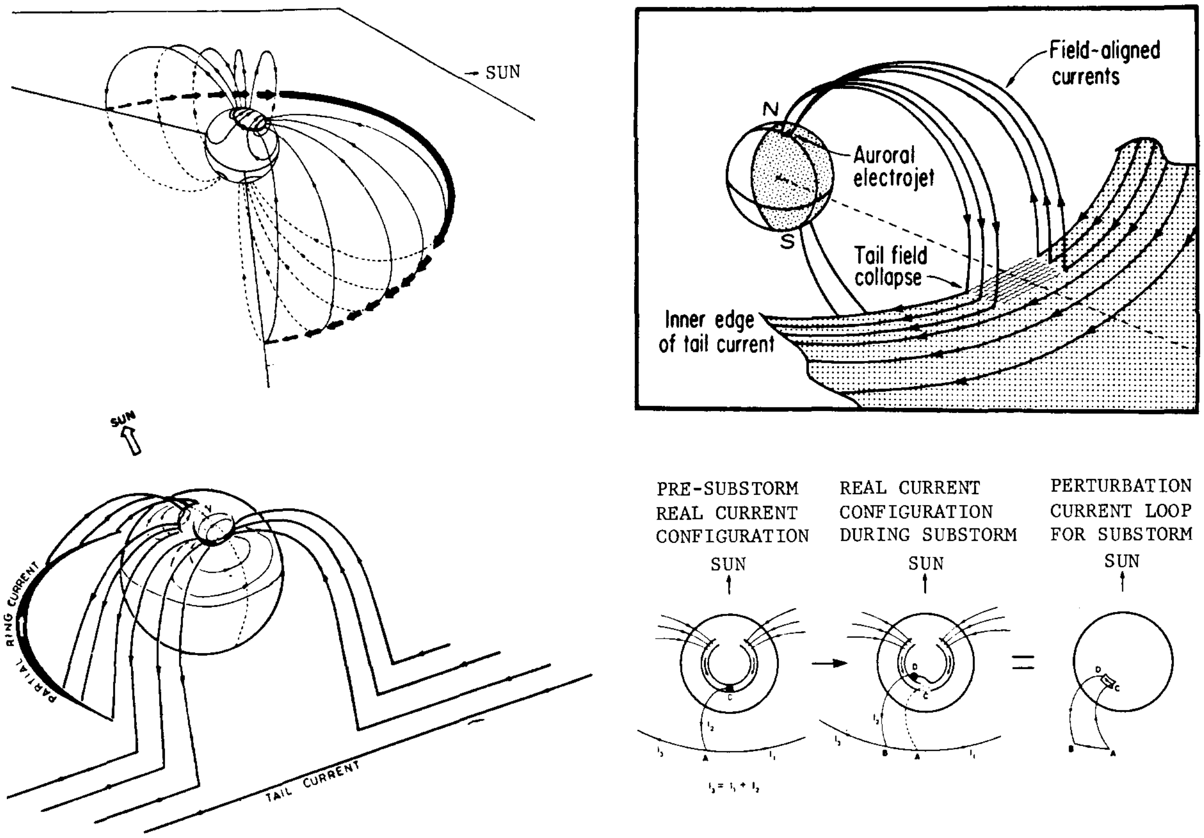

Fig. 4. Ring and field-aligned current models proposed by: (top left) Akasofu and Meng (1969); (top right) McPherron et al. (1973); (bottom left) Kamide and Fukushima (1972); and (bottom right) Rostoker (1974).

three-dimensional real current loop, as ground-based measurements can only give an equivalent current model.

It must be remembered that the equatorial Dst index is simply an approximate parameter to show the ring-current behavior with respect to the storm time. A large negative value of the index is caused by both an increase of current intensity and an earthward shift of the current location. The intensity changes and location shifts are controlled by both local and storm times. Furthermore, a dynamo action by the midlatitude neutral wind caused by the temperature increase in the polar cap and the auroral region is plausible (e.g. Fedder and Banks, 1972; Richmond and Matsushita, 1975). When the heated lower thermospheric air in the auroral region ascends and flows outward at ionospheric F-layer heights a poleward neutral wind in the dynamo region may flow in midlatitudes to complete the circulation, and produce westward electric currents which contribute to a Dst-like decrease of the H component, at least in the daytime, because of a high electric conductivity. In fact, strong poleward neutral winds during storms at 95–100-km altitude over Fritz Peak (g.g. 39.8°N, 105.5°W) have been inferred from measurements of the Doppler shift of the airglow [OI] 5577A emission line (Hernandez and Matsushita, 1974). To discuss the external Dst field, westward electric currents in the dynamo region may need to be considered.

In conclusion, among the slowly-varying external fields, both Sq and Dst seem to have sources in the magnetosphere and the ionosphere, while L seems to be produced mainly in the ionosphere. The classic ideas that the Sq field is simply caused by electric current produced by the wind dynamo in a thin spherical-shell-shaped dynamo region and that the Dst field is produced by a symmetric westward ring current are very misleading for the study of electromagnetic induction in the earth.

Acknowledgements

The author is grateful to Dr. W.H. Campbell, Dr. T.E. Holzer, and Dr. A.D. Richmond for their helpful discussions and to Mrs. R.C. Lyons for her assistance. The National Center for Atmospheric Research is sponsored by the National Science Foundation.

References

Akasofu, S.-I. and Meng, C.-I., 1969. A study of polar magnetic substorms. J. Geophys. Res., 74: 293–313

Alleyne, H., Keenliside, W., Kent, G.S., MacDougall, J.W. and Scholefield, A.J., 1974. Observations of atmospheric tides over Kingston, Jamaica, using three different techniques. J. Atmos. Terr. Phys., 36: 171–175

Amayenc, P., 1974. Tidal oscillations of the meridional neutral wind at midlatitudes. Radio Sci., 9: 281–293

Amayenc, P. and Reddy, C.A., 1972. Height structure of tidal winds as inferred from incoherent scatter observations. Planet. Space Sci., 20: 1269–1279

Amayenc, P. and Vasseur, G., 1972. Neutral winds deduced from incoherent scatter observations and their theoretical interpretation. J. Atmos. Terr. Phys., 34: 351–364

Balsley, B.B., 1973. Electric fields in the equatorial ionosphere: A review of techniques and measurements. J. Atmos. Terr. Phys., 35: 1035–1044

Behnke, R.A. and Hagfors, T., 1974. Evidence for the existence of nighttime F-region polarization fields at Arecibo. Radio Sci., 9: 211–216

Behnke, R.A. and Harper, R.M., 1973. Vector measurements of F region ion transport at Arecibo. J. Geophys. Res., 78: 8222–8234

Bernard, R., 1974. A comparison between meteoric radar and incoherent scatter measurements in the lower thermosphere. Radio Sci., 9: 295–300

Carpenter, D.L. and Seely, N.T., 1974. Some features of quiet-time cross-L plasma drifts in the magnetosphere. Eos, 55: 394

Carpenter, D.L. and Seely, N.T., 1975. Cross-L plasma drifts in the outer plasmasphere; quiet-time patterns and some substorm effects. J. Geophys. Res., 80 (in press)

Coroniti, F.V., 1973. The ring current and magnetic storms. Radio Sci., 8: 1007–1011

Evans, J.V., 1972a. Measurements of horizontal drifts in the E and F regions at Millstone Hill. J. Geophys. Res., 77: 2341–2352

Evans, J.V., 1972b. Ionospheric movements measured by incoherent scatter: A review. J. Atmos. Terr. Phys., 34: 175–209

Fambitakoye, O., Rastogi, R.G., Tabbagh, J. and Vila, P., 1973. Counter-electrojet and Esq disappearance. J. Atmos. Terr. Phys., 35: 1119–1126

Fedder, J.A. and Banks, P.M., 1972. Convection electric fields and polar thermospheric winds, J. Geophys. Res., 77: 2328–2340

Fellous, J.L., Spizzichino, A., Glass, M. and Massebeuf, M., 1974. Vertical propagation of tides at meteor heights. J. Atmos. Terr. Phys., 36: 385–396

Fukushima, N. and Kamide, Y., 1973a. Contribution of magnetospheric field-aligned current to geomagnetic bays and Sq fields: A comment on partial ring-current models. Radio Sci., 8: 1013–1017

Fukushima, N. and Kamide, Y., 1973b. Partial ring current models for worldwide geomagnetic disturbances. Rev. Geophys. Space Phys., 11: 795–853

Hernandez, G. and Matsushita, S., 1974. Lower thermosphere neutral winds. In: S. Matsushita and L.G. Smith (Editors), Proc. Int. Conf. on the E Region. NCAR, Boulder, Colo., pp. 158–164

Hutton, R. and Oyinloye, J.O., 1970. The counter-electrojet in Nigeria. Ann. Géophys., 26: 921–926

Jaggi, R.K. and Wolf, R.A., 1973. Self-consistent calculation of the motion of a sheet of ions in the magnetosphere. J. Geophys. Res., 78: 2852–2866

Kamide, Y., 1974. Association of DP and DR fields with the interplanetary magnetic field variation. J. Geophys. Res., 79: 49–55

Kamide, Y. and Fukushima, N., 1972. Positive geomagnetic bays in evening high-latitudes and their possible connection with partial ring current. Rep. Ionos. Space Res. Jpn., 26: 79–101

Kane, R.P., 1974. Relationship between interplanetary plasma parameters and geomagnetic Dst. J. Geophys. Res., 79: 64–72

Kato, S., 1971. Wave dynamics in the thermosphere: 1. Tidal motion. Space Sci. Rev., 12: 421–445

Kirchhoff, V.W.J.H. and Carpenter, L.A., 1975. Dominance of the diurnal mode of horizontal drift velocities at F region heights. J. Atmos. Terr. Phys., 37: 419–428

Kokubun, S., 1972. Relationship of interplanetary magnetic field structure with development of substorm and storm main phase. Planet. Space Sci., 20: 1033–1049

Lindzen, R.S. and Chapman, S., 1969. Atmospheric tides. Space Sci. Rev., 10: 3–188

Maeda, H., 1955. Horizontal wind systems in the ionospheric E region deduced from the dynamo theory of the geomagnetic Sq variation. J. Geomagn. Geoelectr., 7: 121–132.

Maeda, H., 1963. World-wide pattern of ionization drifts in the ionospheric F region as deduced from geomagnetic variations. In: Proc. Int. Conf. on the Ionosphere. Institute of Physics and Physical Society, London, pp. 187–190

Malin, S.R.C., 1973. Worldwide distribution of geomagnetic tides. Philos. Trans. R. Soc. London, 274: 551–594

Matsushita, S., 1967a. Solar quiet and lunar daily variation fields. In: S. Mastushita and W.H. Campbell (Editors), Physics of Geomagnetic Phenomena. Academic Press, New York, N.Y., pp. 301–424
Matsushita, S., 1967b. Geomagnetic disturbances and storms. In: S. Matsushita and W.H. Campbell (Editors), Physics of Geomagnetic Phenomena. Academic Press, New York, N.Y., pp. 793–819
Matsushita, S., 1968. Sq and L current systems in the ionosphere. Geophys. J. R. Astron. Soc., 15: 109–125
Matsushita, S., 1969. Dynamo currents, winds, and electric fields. Radio Sci., 4: 771–780
Matsushita, S., 1971. Interactions between the ionosphere and the magnetosphere for Sq and L variations. Radio Sci., 6: 279–294
Matsushita, S., 1972. Ionospheric F2 motions interacting with the Sq and L fields. Space Res., 12: 1087–1093
Matsushita, S., 1973. Solar and lunar tidal effects on the low-latitude ionosphere – A review. J. Atmos. Terr. Phys., 35: 1027–1034
Matsushita, S., 1974. The geomagnetic field of external origin as observed at the earth's surface: Ionospheric sources. Eos, 55: 591–593
Matsushita, S. and Campbell, W.H., 1972. Lunar semidiurnal variations of the geomagnetic field determined from the 2.5-min data scalings. J. Atmos. Terr. Phys., 34: 1187–1200
Matsushita, S. and Maeda, H., 1965. On the geomagnetic solar quiet daily variation field during the IGY. J. Geophys. Res., 70: 2535–2558
Matsushita, S. and Mozer, F.S., 1973. Origin of currents and electric fields in the dynamo region. Space Res., 13: 397–412
Matsushita, S. and Tarpley, J.D., 1970. Effects of dynamo-region electric fields on the magnetosphere. J. Geophys. Res., 75: 5433–5443
Matsushita, S., Tarpley, J.D. and Campbell, W.H., 1973. IMF sector structure effects on the quiet geomagnetic field. Radio Sci., 8: 963–972
Matuura, N., 1974. Electric fields deduced from the thermospheric model. J. Geophys. Res., 79: 4679–4689
McPherron, R.L., Russell, C.T. and Aubry, M.P., 1973. Satellite studies of magnetospheric substorms on August 15, 1968: 9. Phenomenological model for substorms. J. Geophys. Res., 78: 3131–3149
Murata, H., 1974. An estimation of the electric potential field generated by the diurnal atmospheric tide with the first negative mode excited in the lower ionosphere. Planet. Space Sci., 22: 569–582
Onwumechili, A. and Akasofu, S.-I., 1972. On the abnormal depression of Sq(H) under the equatorial electrojet in the afternoon. J. Geomagn. Geoelectr., 24: 161–173
Pratap, R., Sarabhai, V. and Nair, K.N., 1973. Three dimensional dynamo theory in the magnetosphere. Astrophys. Space Sci., 20: 307–327
Rastogi, R.G., 1974. Westward equatorial electrojet during daytime hours. J. Geophys. Res., 79: 1503–1512
Richmond, A.D., 1973a. Equatorial electrojet, 1. Development of a model including winds and instabilities. J. Atmos. Terr. Phys., 35: 1083–1103
Richmond, A.D., 1973b. Equatorial electrojet, 2. Use of the model to study the equatorial ionosphere. J. Atmos. Terr. Phys., 35: 1105–1118
Richmond, A.D., 1974. The computation of magnetic effects of field-aligned magnetospheric currents. J. Atmos. Terr. Phys., 36: 245–252
Richmond, A.D. and Matsushita, S., 1975. Thermospheric response to a magnetic substorm. J. Geophys. Res., 80 (in press)
Rishbeth, H., 1971. The F-layer dynamo. Planet. Space Sci., 19: 263–267
Rostoker, G., 1974. Current flow in the magnetosphere during magnetospheric substorms. J. Geophys. Res., 79: 1994–1998
Schieldge, J.P., Venkateswaran, S.V. and Richmond, A.D., 1973. The ionospheric dynamo and equatorial magnetic variations. J. Atmos. Terr. Phys., 35: 1045–1061
Siscoe, G. and Crooker, N., 1974a. A theoretical relation between Dst and the solar wind merging electric field. Geophys. Res. Lett., 1: 17–19
Siscoe, G.L. and Crooker, N.U., 1974b. On the partial ring current contribution to Dst. J. Geophys. Res., 79: 1110–1112
Smith, P.H. and Hoffman, R.A., 1974. Direct observations in the dusk hours of the characteristics of the storm time ring current particles during the beginning of magnetic storms. J. Geophys. Res., 79: 966–971
Stening, R.J., 1969. An assessment of the contributions of various tidal winds to the Sq current system. Planet. Space Sci., 17: 889–908
Stening, R.J., 1970. Tidal winds and the Sq current system. Planet. Space Sci., 18: 121–122
Stening, R.J., 1973. The electrostatic field in the ionosphere. Planet. Space Sci., 21: 1897–1910
Sugiura, M. and Chapman, S., 1960. The average morphology of geomagnetic storms and sudden commencements. Abh. Akad. Wiss. Göttingen, Math.-Phys. Kl., Sonderh. 4, 1–53
Suzuki, A., 1973a. Returning flow of the equatorial electrojet currents. J. Geomagn. Geoelectr., 25: 249–258
Suzuki, A., 1973b. A new analysis of the geomagnetic Sq field. J. Geomagn. Geoelectr., 25: 259–280
Tarpley, J.D., 1970a. The ionospheric wind dynamo, 1. Lunar tide. Planet. Space Sci., 18: 1075–1090
Tarpley, J.D., 1970b. The ionospheric wind dynamo, 2. Solar tides. Planet. Space Sci., 18: 1091–1103
Tarpley, J.D., 1971. The O_1 component of the geomagnetic lunar daily variation. J. Geomagn. Geoelectr., 23: 169–179
Tarpley, J.D., 1973. Seasonal movement of the Sq current foci and related effects in the equatorial electrojet. J. Atmos. Terr. Phys., 35: 1063–1071
Tarpley, J.D. and Balsley, B.B., 1972. Lunar variations in the Peruvian electrojet. J. Geophys. Res., 77: 1951–1960
Taylor, G.N., 1974. Meridional F2-region plasma drifts at Malvern. J. Atmos. Terr. Phys., 36: 267–286

Volland, H. and Mayr, H.G., 1972. A three-dimensional model of thermosphere dynamics. J. Atmos. Terr. Phys., 34: 1745–1816
Volland, H. and Mayr, H.G., 1973. A numerical study of three-dimensional diurnal variations within the thermosphere. Ann. Géophys., 29: 61–75
Volland, H. and Mayr, H.G., 1974. Tidal waves within the thermosphere. Radio Sci., 9: 263–273
Winch, D.E., 1970. Geomagnetic lunar tides, O_1 component. J. Geomagn. Geoelectr., 22: 319–328
Woodman, R.F., 1970. Vertical drift velocities and east–west electric fields at the magnetic equator. J. Geophys. Res., 75: 6249–6259
Yabuzaki, T. and Ogawa, T., 1974. Rocket measurement of Sq ionospheric currents over Kagoshima, Japan. J. Geophys. Res., 79: 1999–2001